Modeling of transport phenomena in a fuel cell anode

Frank A. Coutelieris

Department of Engineering and Management of Energy Resources,
University of Western Macedonia, Bakola & Sialvera, 50100 Kozani, Greece,
Tel: +302461056751; Fax: +302461021731; e-mail: fcoutelieris@uowm.gr

and

National Center for Scientific Research "Demokritos", 15310 Aghia Paraskevi Attikis, Greece, Tel: +302106503447; Fax: +302106525004; e-mail: frank@ipta.demokritos.gr

Keywords: SOFC, anode; catalyst layer; heat transfer; mass transport.

Abstract A mathematical model for the simulation of the transport phenomena occurred in the anode of a typical fuel cell is presented here. The model initially considers a simple one-dimensional geometry where the mass transport equation is combined with a Tafel-type description for the current density. By assuming isothermal conditions, the numerical solution of the differential equations was achieved with the use of a non-linear shooting scheme in conjunction with the multidimensional Newton algorithm. The space was discretized through a constant-step mesh while the resulting nonlinear system of ordinary differential equations was solved by using the 4th order Runge-Kutta method. The whole algorithm was implemented by developing a new FORTRAN code. In addition, a planar two-dimensional geometry is also considered, where the mass transport is described by the convection-diffusion equation within the catalyst layer together with the Navier-Stokes equation for laminar flow conditions and the electrochemical effects, while the convective heat transfer within the developed diffusion layer is also taken into account. This approach has been numerically implemented and solved by using the finite volume method being applicable through the CFD-RC© commercial package. For the sake of simplicity, the feedstream of the fuel cell was assumed to be a hydrogen-rich mixture (H_2 >90%) for all cases. Both SOFC and PEM type fuel cells were considered in this study, while the results are presented in terms of fuel concentration, produced current density and overpotential.

Introduction

During the last years, fuel cells have attracted considerable scientific and engineering interest because they present high efficiency and very low environmental impact. It is important that various fuel options such as natural gas, methanol, ethanol and gasoline are considered feasible for fuel cell operation, offering a very significant ecological dimension in the problem of effective energy conversion [1]. Several types of fuel cells have been investigated and applied till nowadays, among which Solid Oxide Fuel Cells (SOFCs) and Polymer Electrolyte Membrane Fuel Cells (PEMFCs) have attained the wider acceptance in terms of applications [2]. The mass transport within a fuel cell is a key factor to its performance. Especially, PEM-type fuel cell suffers from mass transport limitations predominantly at anode, arising from the diffusion of fuel in covering the active electrocatalyst layer and from hydrodynamics in the anode flow channel. The geometrical characteristics of the electrodes (thickness, volume porosity, tortuosity etc) are the crucial parameters affecting the mass transport of chemical species through the electrode/electrolyte

interface. This process influences significantly the overpotential, therefore the efficiency of the cell in terms of power production, mainly because of temperature singularities [2, 3].

Since there are serious difficulties in realizing prototypes, numerous multi-dimensional simulation have been published because mathematical modeling is essential for the better understanding of the role of the main parameters that affect the performance of a fuel cell [4-6]. Most of these studies have been focused on the anode of the cell, because this is the place where the electrochemical reactions occur, thus it might play the most important role in the power production process. Among these simulation activities, the most simple and interesting model is that of Jeng and Chen [7] and Jeng et al. [8], who managed to predict the behavior of a direct methanol PEM fuel cell, while the effect of the current density on fuel crossover was also examined. Their one-dimensional approach is very important because it is quite trouble-free, accurate and easily applicable to other configurations, although it suffers from some uncertainties (for example, they assumed that methanol concentration in the diffusion layer is insignificant compared with that of water).

In the present work, the above mentioned 1-D approach was used in order to develop a predictive mathematical model for the transport phenomena occurring along the axis of a generic typical fuel cell anode. Obviously, a significant trial to overcome some of the above mentioned deficiencies has been incorporated here. Further to this simple modeling approach, a more detailed 2-D simulation has also been implemented for the same processes in order to overcome superficial assumptions and mathematical manipulations. A comparison between these two approaches, being applied to both SOFC and PEM fuel cell configurations, is also presented with the purpose to further investigate the value added by the two-dimensional approach.

Model description

The operation of a typical fuel cell is based on the continuous supply of its anode by a hydrogen-rich fuel mixture while cathode is exposed to atmospheric air. In any case, the produced ions migrate trough electrolyte and heterogeneously react in order to produce water, heat and power. More precisely, the reactions that take place in a fuel cell are as follows

Fuel cell type	Place	Reaction	
SOFC	Cathode	$O_2 + 4e^- \rightarrow 2O^{2-}$	(1a)
SOFC	Anode	$H_2 + O^{2-} \rightarrow H_2O + 2e^-$	(2a)
PEM	Anode	$2H_2 \rightarrow 4H^+ + 4e^-$	(1b)
PEM	Cathode	$O_2 + 4H^+ + 4e^- \rightarrow 2H_2O$	(2b)

A typical 2-D cut of a fuel cell containing the anode area is schematically presented in Fig. 1. In particular, anode is divided into three regions: an electrolyte region, an active catalyst region (catalyst layer) that provides a catalytic site for the oxidation of fuel and a diffusion region (diffusion layer) composed of highly porous and electronically conductive material. The electrolyte is assumed to be dense in the case of SOFC and porous for the case of PEM fuel cell. The diffusion layer is located adjacent to the flow channel and favoring the distribution of reactants to the catalyst layer. For the modeling point of view, the area of interest is the catalyst layer. The fuel fed to the anode compartment of the fuel cell is assumed to be a mixture of high hydrogen content (H_2 >90%). It is also assumed that hydrogen reacts only partially in the catalyst/electrolyte interface; therefore a remaining portion follows the stream to the outlet and/or crossovers to the cathode compartment.

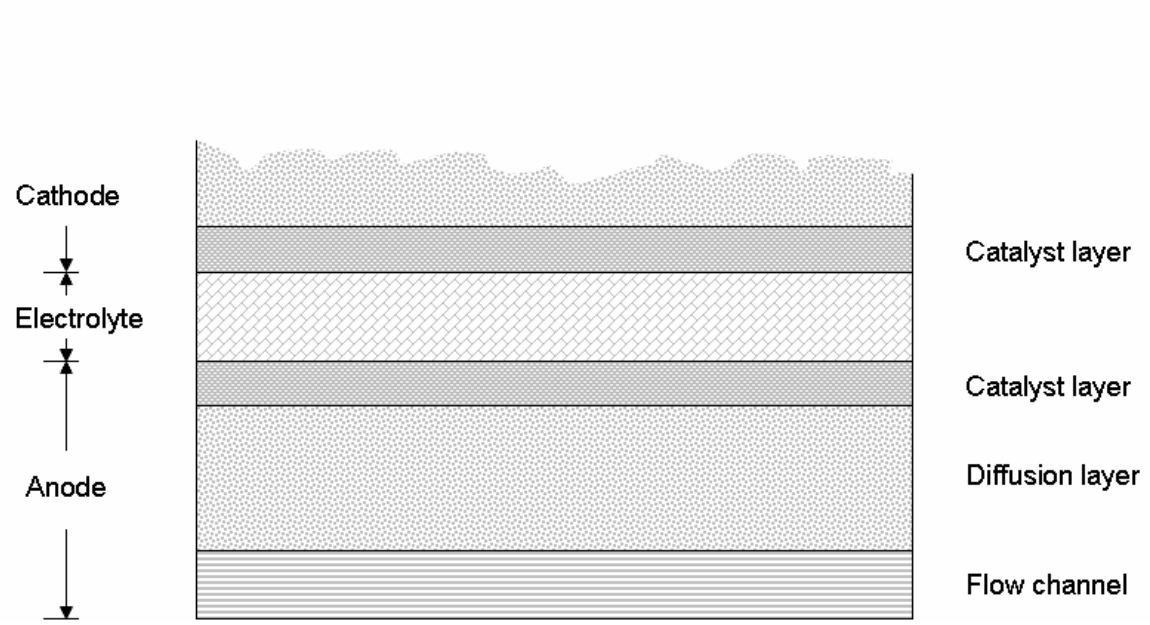

Figure 1: Schematic diagram of the simulated (anode) area.

One dimensional model

By assuming that the pressure in both anode and cathode compartments is equal to 1 atm and that the major transport processes mainly occur at the direction parallel to the cell axis, the mass flux in the catalyst layer for steady-state isothermal conditions can be expressed as follows

$$j_f = -D_f^{eff} \frac{dC_f}{dx} + C_f j_w \tag{3}$$

where D_f^{eff} is the effective diffusivity of fuel in the catalyst layer and j_f, j_w are the mass fluxes of the fuel and the water, respectively. In the above equation, the convection term has been neglected since the velocity is very low within the catalyst layer [7, 8]. By taking into account the material balance for the water, its mass flux is given as

$$j_w = j_w^d + \frac{I - i}{4F} \tag{4}$$

where $\frac{I - i}{4F}$ is the flux of the produced water mass and j_w^d represents the water flux entering the catalyst through the diffusion layer. By I and i the cell and ionic current density are denoted, respectively, while F represents the Faraday's constant. The water flux from diffusion layer depends on fuel cell type, being zero in the case of SOFC , i.e.

$$j_w^d = 0 \tag{5a}$$

For the case of PEM fuel cell, the above mentioned mass flux is approximated as [7]

$$j_w^d = \lambda_w^d \frac{I}{F} \tag{5b}$$

where λ_w^d is the electro-osmotic drag coefficient of water. It is worth noticing that the oxidation of fuel along the axis of the fuel cell is linear with the ionic current density, thus the variation of mass flux is analogous to the spatial evolution of current density, i.e.

$$\frac{dj_f}{dx} = -\frac{1}{4F}\frac{di}{dx} \tag{6}$$

By differentiating eq. (3) and using eqs. (5b) and (6), the governing differential equation for mass transfer within the catalyst layer becomes as follows

$$D_f^{eff}\frac{d^2C_f}{dx^2} = \left(\frac{I-i}{4F} + \lambda_w^d\frac{I}{F}\right)\frac{dC_f}{dx} + \frac{I}{4F}\left(1-C_f\right)\frac{di}{dx} \tag{7a}$$

which is valid for the case of PEM fuel cell. When a SOFC is considered, it becomes

$$D_f^{eff}\frac{d^2C_f}{dx^2} = \frac{I-i}{4F}\frac{dC_f}{dx} + \frac{I}{4F}\left(1-C_f\right)\frac{di}{dx} \tag{7b}$$

Since the last equations combine the mass transport with the local current density, it is necessary to develop the relative expression for i. Starting from the well known Butler-Volmer equation and after same simplifications, a Tafel-type equation can be obtained

$$\frac{di}{dx} = K\left(C_f\right)^{\gamma} e^{\frac{4a_aF}{RT}\eta} \tag{8}$$

where γ is the order of the reaction, η is the anodic overpotential and K is a coefficient including the geometrical and physical properties of the electrolyte. By involving the local potentials at catalyst layer and at ionomeric phase as well as the Ohm's law, the variation of the overpotential within the catalyst layer is given as [7, 8]

$$\frac{d\eta}{dx} = \left(R_m + R_s\right)i - R_s I \tag{9}$$

where R_m is the effective ionic resistance in the catalyst layer and R_s is the effective resistance in the solid phase.

Again, by differentiating eq. (8) and using eq. (9), it is easy to obtain the governing differential equation for current density within the catalyst layer as follows

$$\frac{d^2 i}{dx^2} = \left\{ \frac{\gamma}{C_f} \frac{dC_f}{dx} + \frac{4a_a F}{RT} \left[\left(R_m + R_s \right) i - R_s I \right] \right\} \frac{di}{dx} \tag{10}$$

In order to numerically integrate the system of either eqs. (7a) & (10) or eqs. (7b) & (10), it is necessary to decrease the order by introducing new unknowns C_f^* and i^* (downgrade technique), thus a system of four equations is produced for the case of PEM as follows

$$\frac{dC_f}{dx} = C_f^* \tag{11a}$$

$$\frac{di}{dx} = i^* \tag{11b}$$

$$\frac{dC_f^*}{dx} = \frac{1}{4FD_f^{eff}} \left[\left(I - i + 4\lambda_w^d I \right) C_f^* + I \left(1 - C_f \right) i^* \right] \tag{11c}$$

$$\frac{di^*}{dx} = \left\{ \frac{\gamma}{C_f} C_f^* + \frac{4a_a F}{RT} \left[\left(R_m + R_s \right) i - R_s I \right] \right\} i^* \tag{11d}$$

Note that eq. (11c) becomes for the case of SOFC

$$\frac{dC_f^*}{dx} = \frac{1}{4FD_f^{eff}} \left[\left(I - i \right) C_f^* + I \left(1 - C_f \right) i^* \right] \tag{11e}$$

Independently on the fuel cell type, the boundary conditions accompanying the above system are as follows

$$C_f^* \left(x = 0 \right) = 0 \tag{12a}$$

$$C_f \left(x = 0 \right) = C_f^{ref} \tag{12b}$$

$$i \left(x = 0 \right) = 0 \tag{12c}$$

$$i^* \left(x = 0 \right) = 0 \tag{12d}$$

where C_f^{ref} is the uniform reference fuel concentration at the inlet. Although it is rather obvious that

$$i \left(x = cell\ length \right) = I \tag{13}$$

the analysis here does not use the relation above for the description of the boundary condition as in [7], because it is better for the accurate convergence of a first order system of differential equations to be accompanied by initial conditions at the same point of the domain [9]. Therefore, the above eq. (13) is considered as one of the criteria against which the solution of the system must be evaluated.

The numerical solution of the systems of differential equations (11a), (11b), (11c)/(11e) and (11d) was achieved with the use of a non-linear shooting scheme in conjunction with the multidimensional Newton algorithm [10]. The space was discretized through a constant-step mesh, while the resulting nonlinear system of ordinary differential equations was solved by using the 4th order Runge-Kutta method. A new FORTRAN code was developed to implement the above mentioned numerical scheme, while the values used are as in [7] and [8]. The computational time in a simple home PC is of order of seconds, depended on the initial guesses for the Newton method.

Two dimensional model

The configuration of a typical planar fuel cell is as in Fig. 2 where the simulated area has been divided in seven separate regions: the anode and the cathode channel, the porous anode and cathode, the electrolyte layer and the two contacts. The fuel and air mixtures enter the system through the anode and cathode channel respectively and have typical compositions.

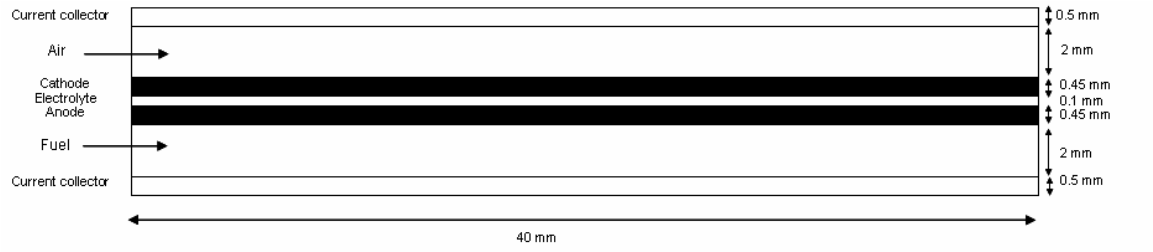

Figure 2: Simulated geometry f a planar fuel cell

The steady state laminar flow is studied by using the Navier-Stokes equation for incompressible fluids

$$\underline{u}\cdot\nabla\left(\rho\underline{u}\right)=-\nabla p+\mu\nabla^2\underline{u} \tag{14}$$

where $\underline{u}$ is the local velocity vector, ρ is the density, p is the pressure, and μ is the viscosity. All these quantities are referred to the mixture of both the anodic and cathodic feed-stream.

By neglecting the radiation term, the heat transfer equation in the fuel cell becomes as follows

$$\underline{u}\cdot\nabla\left(\rho c_p T\right)=\dot{Q}+\nabla\cdot a\nabla\left(\rho c_p T\right)-\rho c_p T\nabla\cdot\underline{u} \tag{15}$$

where c_p is the mixture's specific heat, a is the diffusion thermal coefficient and $\dot{Q}$ is the produced or consumed heat.

Since only surface reactions are taken into account for the current simulations (no-bulk reactions), the mass transport equation is of the form

$$\underline{u} \cdot \nabla C_i - \nabla \cdot \left(D_{i,mix} \nabla C_i \right) = 0 \tag{16}$$

where C_i is the concentration of i-species and $D_{i,mix}$ is the diffusion coefficient of this component in the mixture.

By assuming charge transfer controlled process, the Butler-Volmer equation has been incorporated for the electrochemical reactions occurring in the cell and the calculation of current density, as

$$i = i_0 \left[\exp\left(\frac{a_a F}{RT} \eta \right) - \exp\left(-\frac{a_c F}{RT} \eta \right) \right] \tag{17}$$

where i_0 is the exchange current density, a_a and a_c are the anodic and cathodic charge transfer coefficients, respectively, and R is the ideal gas constant.

For the simulations presented here, constant values of mass inflow rates were used for both the anode and the cathode channel mixtures and fixed pressure boundary condition of 1 atm was set to both outlets. A voltage of 0.73 V was applied to the cathode contact and the boundary condition for the temperature was assumed isothermal and fixed to 1073 K for the case of SOFC and 373K for the case of PEM. All the other boundary conditions were set to wall indication with zero value of velocity, zero flux of temperature, species composition and current indication.

In order to achieve the numerical solution of the above equations, a 2-D mesh was developed in accordance with the specific dimensions as in Fig. 2. The finite volume method was used through the commercially available software package CFD-RC© for the solution of eqs. (14)-(17) where the simulated domain was discretized by an unstructured grid. The values of the operational parameters are as in [7], [8], [11] and [12]. In order to achieve residual values lower than 10^{-4} for all the unknown quantities, a computational time of approximately half an hour was on average necessary for runs on an Intel Pentium 3.2 GHz computer.

Results and Discussion

The hydrogen molar fraction obtained by the one-dimensional model as function of dimensionless normalized length is presented in Fig. 3 for various current densities. As expected [1], concentration decreases with the current density. It is also depicted that the concentration profiles are nearly linear for low current densities, because diffusion dominates at this conditions, therefore only a small portion of hydrogen is consumed in the catalyst layer. Finally, SOFC configuration presents significantly higher hydrogen concentrations than those of PEM, because the membrane is permeable allowing a portion of hydrogen to escape towards the cathode's side. This is

not possible for the case of the dense electrolyte of a SOFC, presenting a zero additional water flux (see eqs. 5a & 5b). The comparison between the two different fuel cell types is more clearly presented in Fig. 4, where the same results as those of Fig. 3 have been obtained by the two-dimensional approach. Hydrogen is consumed with higher rates in the case of PEM, thus producing higher heat amounts, as well as more power.

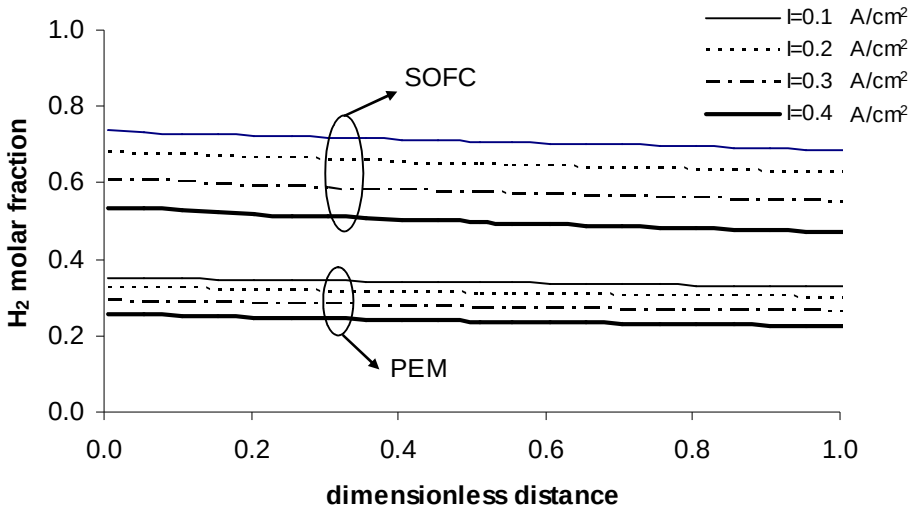

Figure 3: Hydrogen concentration within the catalyst layer for various current densities

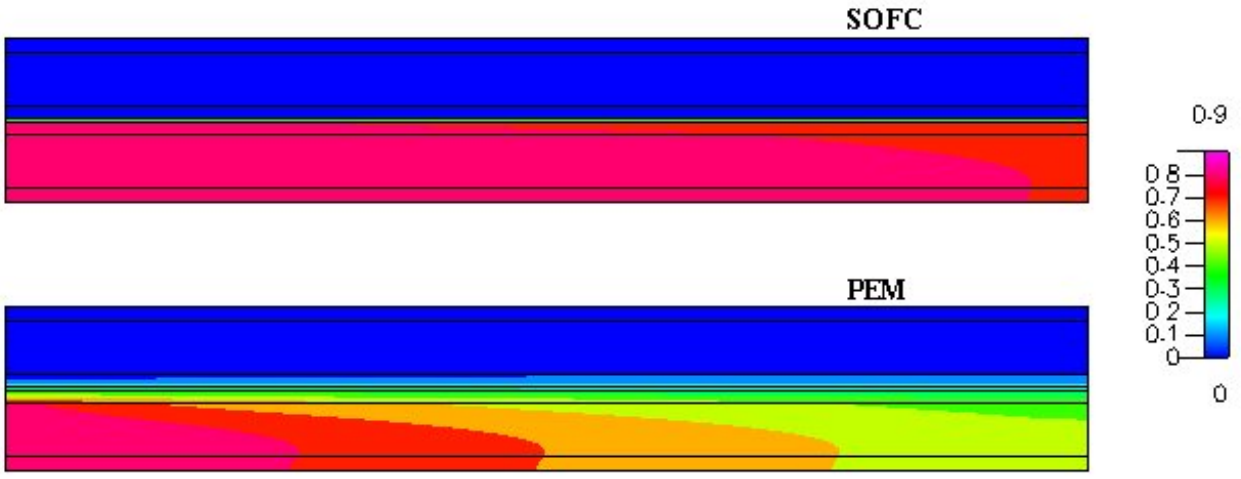

Figure 4: Hydrogen concentration for SOFC and PEM configurations

Fig. 5 presents the overpotential in the catalyst layer as estimated by the 1-D approach. As above, several values of current density and two fuel cell types have also been considered. A rather smooth increment from the inlet to the outlet is observed (note the scale of y-axis), resulted by the consequent increment of the hydrogen consumption with the distance, as it has been shown in Fig. 3. Furthermore, the overpotential increases with current density, which is in accordance with previously presented experimental and theoretical results [7, 8, 11, 12]. It is important to note that overpotential values at the inlet area are not exactly zero since some consumption of hydrogen

already exists in the diffusion layer for both SOFC and PEM cells. Finally, it is important to note that SOFC always presents slightly higher overpotential values than those of PEM, mainly because of the higher operational temperature of the cell. However, this difference can be characterized as insignificant since it is les than 0.05V for the same conditions. The same qualitative behavior is also observed in Fig. 6, where relative results from 2-D model are presented. In terms of quantitative analysis, the overpotential values are to some extent different (higher) than those of Fig. 5, because of the most detailed model, being closer to elsewhere obtained overpotential [11, 12] than 1-D respective results of Fig. 6.

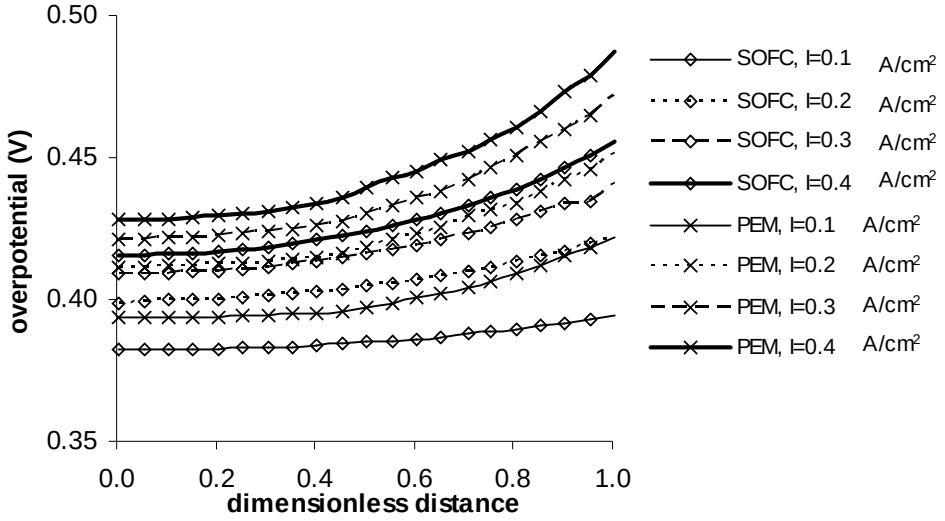

Figure 5: Overpotential within the catalyst layer for various current densities

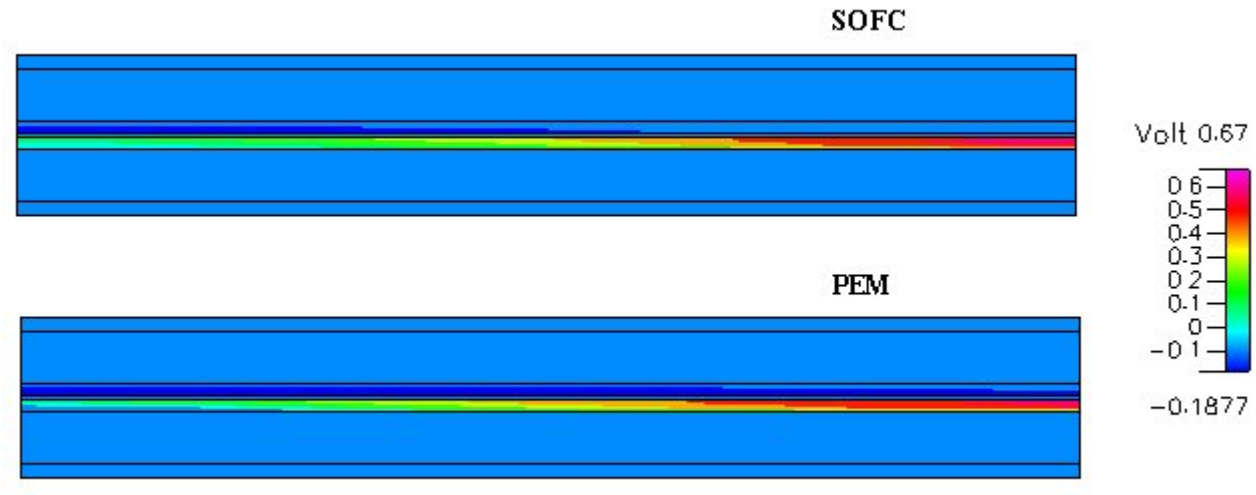

Figure 6: Overpotential for SOFC and PEM configurations

Conclusions

In the present work, two approaches have been adopted to adequately simulate the transport phenomena occurred in the anode of a fuel cell. The first one is a one dimensional, relatively simple model, which is analogous to those presented in [7] and [8]. Such a model should involve some assumptions (like isothermal operation, pre-defined current at outlet, etc.) to obtain the 1-D

solution. To overcome such theoretical issues, a more complicated two-dimensional approach has also been developed, including the coupled solution for flow, heat transfer, mass transport and electrochemistry. It is found that both models describe with sufficient accuracy [11, 12] the operation of a fuel cell in terms of feedstock concentration and overpotential produced. By using both the approaches, SOFC and PEM configurations were compared and a slight advantage of SOFC has been underlined, since it presents higher fuel consumption as well as higher overpotential values.

Acknowledgment

Author would like to thank Mrs. Eleni Vakouftsi for her technical assistantship in CFD-RC© issues and Mr. Dimitrios Sarantarides for some fruitful discussions on the topic.

References

[1] Hirschenhofer JH, Stauffer DB, Engleman RR, Klett MG, "Fuel Cell Handbook", 4th Edition ed., Business/Technology Books: Orinda, USA (1997).

[2] R. Sousa, E.R. Gonzalez: J. Power Sources Vol. 147 (2005), p. 32

[3] S.H. Chan, K.A. Khor, Z.T. Xia: J. Power Sources Vol. 93 (2001), p. 130

[4] K. Scott, W. Taama, J. Cruickshank: J. Power Sources Vol. 65 (1997), p. 159

[5] P.R. Pathapati, X. Xue, J. Tang: Renewable Energy Vol. 30 (2005), p. 1

[6] D. Cheddie, N. Munroe: J. Power Sources Vol. 147 (2005), p. 72

[7] K.T. Jeng, C.W. Chen: J. Power Sources, Vol. 112 (2002), p. 367

[8] K.T. Jeng, C.P. Kuo, S.F. Lee: J. Power Sources Vol. 128 (2004), p. 145

[9] Ames WF, "Numerical methods for partial differential equations", Academic Press: New York, USA (1977).

[10] Keller HB, "Numerical methods for two-point boundary-value problems", Blaisdel: Waltham, USA (1968)

[11] Bockris JOM, Reddy AKN, "Modern Electrochemistry", Plenum Press: New York, USA (1997).

[12] P.A. Ramakrishna, S. Yang, C.H. Sohn: J. Power Sources Vol. 158 (2006), p. 378